IEEE TRANSACTIONS ON

ELECTROMAGNETIC COMPATIBILITY

A PUBLICATION OF THE IEEE ELECTROMAGNETIC COMPATIBILITY SOCIETY

EMC SOCIETY

AUGUST 2009 VOLUME 51 NUMBER 3 IEMCAE (ISSN 0018-9375)

PART II OF TWO PARTS

PAPERS

(Contents Continued on Page 573)

IEEE

Celebrating 125 Years
of Engineering the Future

IEEE TRANSACTIONS ON ELECTROMAGNETIC COMPATIBILITY (ISSN 0018-9375) is published quarterly by the Institute of Electrical and Electronics Engineers, Inc. Responsibility for the contents rests upon the authors and not upon the IEEE, the Society/Council, or its members. **IEEE Corporate Office**: 3 Park Avenue, 17th Floor, New York, NY 10016-5997. **IEEE Operations Center:** 445 Hoes Lane, Piscataway, NJ 08854-4141. **NJ Telephone**: +1 732 981 0060. **Price/Publication Information:** Individual copies: IEEE Members $20.00 (first copy only), nonmembers $100.00 per copy. (Note: Postage and handling charge not included.) Member and nonmember subscription prices available upon request. Available in microfiche and microfilm. Periodicals Postage Paid at New York, NY and at additional mailing offices. **Postmaster:** Send address changes to IEEE TRANSACTIONS ON ELECTROMAGNETIC COMPATIBILITY, IEEE, 445 Hoes Lane, Piscataway, NJ 08854-4141. GST Registration No. 125634188. CPC Sales Agreement #40013087. Return undeliverable Canada addresses to: Pitney Bowes IMEX, P.O. Box 4332, Stanton Rd., Toronto, ON M5W 3J4, Canada. Printed in U.S.A.

Digital Object Identifier 10.1109/TEMC.2009.2030264

Correspondence

On HF Circuit Models of Horizontal Grounding Electrodes

L. Grcev, *Senior Member, IEEE*, and S. Grceva

***Abstract*—Inductance to ground in high-frequency circuit models of horizontal grounding electrodes is often "erroneously" approximated by applying image theory. Two other approximate approaches that are often used are based on a transverse electromagnetic propagation assumption and on a homogeneous medium assumption, respectively. We compare these three approaches with an "exact" electromagnetic approach by computing the grounding impedance in scenarios with soil resistivity of 10–1000 Ω·m and electrode length up to 100 m. Surprisingly, the circuit model based on the image theory leads to better results in case of inductive behavior. This is also confirmed by comparison with experimental results.**

***Index Terms*—Circuit modeling, grounding electrodes, lightning, transient response, transmission line (TL) modeling.**

I. Introduction

A horizontal grounding electrode fed by a high-frequency (HF) or impulse current is traditionally simulated by a transmission line (TL) with uniformly distributed parameters [1]. The analysis requires per-unit-length parameters for resistance r (in ohms meter), capacitance c (in farads per meter), and inductance l (in henries per meter), which are usually determined by the quasi-static approximation. The resistance r is usually calculated by [1]

$$r = \frac{\rho}{\pi}\left[\log\frac{2\ell}{\sqrt{2da}} - 1\right], \qquad (\ell \gg a,\ d \ll \ell) \tag{1}$$

where ρ (in ohms meter) is the resistivity of the earth, ℓ (in meters) is the electrode length, a (in meters) is the electrode radius, and d (in meters) is the depth of burial. The formula is derived by applying image theory yielding two equal parallel conductors separated by a distance $2d$ in a homogeneous medium with resistivity ρ. Similarly, the grounding capacitance c is computed by considering the duality relationship between c and $1/r$ [1] by

$$c = \frac{\rho\varepsilon}{r} \tag{2}$$

where ε is the permittivity of the soil in (in farads per meter).

Sunde [1, p. 256] proposed the approximate formula for the inductance l derived for an electrode at the surface (equivalent to an electrode in a homogeneous medium) by

$$l = \frac{\mu}{2\pi}\left[\log\frac{2\ell}{a} - 1\right] \tag{3}$$

where μ (in henries per meter) is the permeability of the soil. This approximation is based on an observation that for horizontal wires at ordinary depths, the inductances are substantially the same as for wires at the surface [1, p. 114].

Manuscript received January 30, 2009; revised April 1, 2009. First published June 26, 2009; current version published August 21, 2009.

L. Grcev is with the Faculty of Electrical Engineering and Information Technologies, Ss. Cyril and Methodius University, Skopje 1000, Macedonia (e-mail: lgrcev@feit.ukim.edu.mk).

S. Grceva is with the Faculty of Informatics, Goce Delcev University, Stip 2000, Macedonia (e-mail: solza.grceva@ugd.edu.mk).

Digital Object Identifier 10.1109/TEMC.2009.2023330

In addition, another approximate formula for the inductance l is derived from the relation based on the transverse electromagnetic (TEM) field assumption [2] as

$$l = \frac{\mu\varepsilon}{c} \tag{4}$$

leading to

$$l = \frac{\mu}{\pi}\left[\log\frac{2\ell}{\sqrt{2da}} - 1\right]. \tag{5}$$

However, (4) is not valid for electrodes below ground, as it is derived for unbounded homogenous medium [2, p. 296].

Yet another approximate approach is based on an analysis where the buried electrode is assumed to have a positive mirror image, e.g., King [3], leading to

$$l = \frac{\mu}{2\pi}\left[\log\frac{2\ell}{\sqrt{2da}} - 1\right]. \tag{6}$$

However, Wait [4] has shown that the image theory does not adequately represent the magnetic field of horizontal grounding electrodes.

Nevertheless, all approaches, i.e., using (3), (5), and (6), have been used and compared with experimental results with fair agreement by a number of authors, e.g., (3) in [5] and [6], (5) in [7] and [8], and (6) in [9] and [10].

To examine the practical importance of the differences in these approaches, we compare their results with an exact analytical model based on electromagnetic (EM) theory [11] for a practical range of parameters and with experimental results. In these comparisons, we do not take into account effects of soil ionization. The application of the model for such effects is discussed, for example, in [7]–[10].

II. Comparison of Results

One of the most important properties in the HF analysis of grounding electrodes is the harmonic impedance to ground Z. It can be computed as the input impedance of an open TL in the frequency domain [12] as

$$Z = Z_0 \coth \gamma\ell \tag{7a}$$

$$Z_0 = \sqrt{\frac{j\omega l}{(1/r + j\omega c)}} \qquad \gamma = \sqrt{j\omega l\left(\frac{1}{r} + j\omega c\right)}. \tag{7b}$$

The most accurate approach to this problem is based on the solution of Maxwell's equations for the given boundary conditions, for example, by the EM model [11]. Olsen and Willis [13, p. 1081] have established this approach, i.e., the integral equation approach involving Sommerfeld's solution solved by the method of moments, as an "exact" solution to this problem and as a "gold standard" for comparison.

Figs. 1 and 2 show simulation results of the modulus of Z (7a) of 10-m- and 100-m-long horizontal electrodes, respectively, by the EM model [11] designated by "EM," the TL model using (3) designated by "TL," the TL model using (5) designated by "TL (TEM)," and the TL model using (6) designated by "TL (image)." The radius of electrodes is 7 mm, the depth of burial is 0.8 m, and the relative permittivity of the earth is 10.

Figs. 1 and 2 show typical frequency-independent behavior in the low-frequency range, where $Z \approx R$ (here R is a DC resistance to ground). At higher frequencies, higher than a certain switch frequency F_C, the behavior is either dominantly inductive, for which $|Z| > R$, or dominantly capacitive, for which $|Z| < R$. Resonant behavior is also typical in the case of the capacitive performance (see Fig. 1, $\rho = 1000\,\Omega{\cdot}$m).

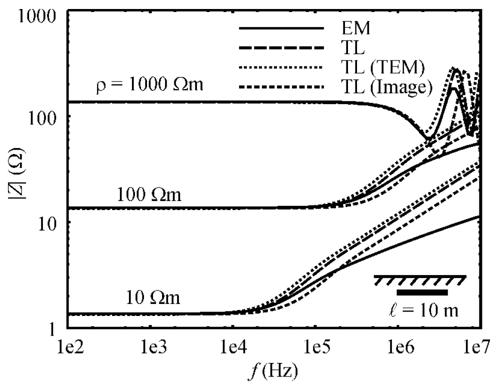

Fig. 1. Harmonic impedance of a 10-m-long horizontal grounding electrode.

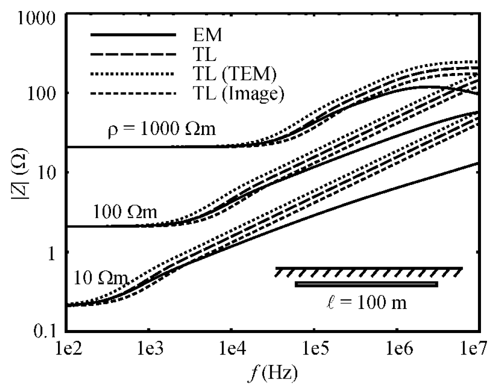

Fig. 2. Harmonic impedance of a 100-m-long horizontal grounding electrode.

It is evident from Figs. 1 and 2 that the computed characteristic frequencies, i.e., the F_C and resonant frequencies, from the TL (TEM) and TL (image) models are not consistent with the EM model. On the other hand, the values of the characteristic frequencies from the TL and EM models are in fair agreement.

In case of inductive behavior, the values of $|Z|$ from all the TL models and the EM model mutually diverge in the HF range. However, the results from the TL (image) model agree somewhat better with the EM model in comparison to the other TL models throughout the HF ranges considered in Figs. 1 and 2. This unexpected result can be linked to the larger value of F_C, and consequently, to smaller values of $|Z|$ at higher frequencies computed from the TL (image) in comparison to the other TL models. In addition, we also note an important irregularity in the TL (image) model, which results in smaller values of $|Z|$ in comparison to the EM model in a limited frequency range above F_C. However, this irregularity may also contribute to better results in time domain, as illustrated in the case in Fig. 3.

On the other hand, in case of capacitive behavior, the TL model (3) generates more accurate results than both the TL (TEM) and TL (image) models in HF range.

To illustrate the possible consequences of the model differences in the time domain, we show in Fig. 3 the measured voltage to ground at the endpoint of an 8-m-long horizontal electrode where fast rise time current pulse is injected [14]. Such a fast rise time pulse, with a zero-to-peak time of about $0.2\,\mu$s, has a large HF content, which is important for testing HF inductive behavior. The time-domain response is computed by the inverse Fourier transform method [11].

The behavior in Fig. 3 is inductive, characterized by a large voltage peak that leads the current pulse. The voltage peak value is best estimated by the EM model. The TL (image) model (6) leads to a better estimate than TL model (3) or TL (TEM) model (5). However, the TL

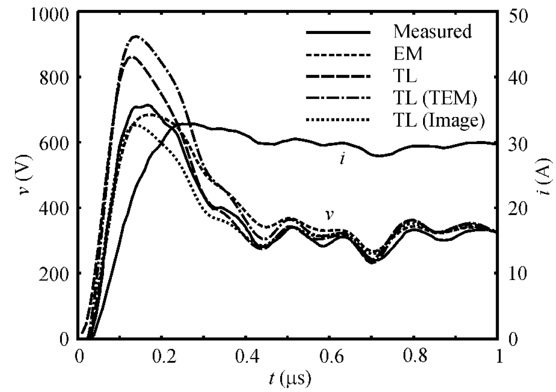

Fig. 3. Comparison with measurements by Electricity de France [14] ($\ell = 8$ m, $a = 6$ mm, $d = 0.8$ m, $\rho = 65\,\Omega\cdot$m, and $\varepsilon_r = 15$).

(image) model unexpectedly generates smaller voltage peak value than the EM model. This effect strongly depends on the parameter values. More specifically, it is a result of a circumstance that the frequency content of the rising portion of the current pulse, which dominantly determines the voltage peak value, overlaps with the frequency range just above F_C where the TL (image) model generates smaller values of $|Z|$ than the EM model.

The analyzed cases illustrate that there exist circumstances when the results from the "erroneous" TL (image) model using (6) might be more consistent with the EM model than the other considered TL models (such as in the case of inductive behavior), and also when this is not the case (such as in the case of capacitive behavior).

REFERENCES

[1] E. D. Sunde, *Earth Conduction Effects in Transmission Systems*, 2nd ed. New York: Dover, 1968.

[2] C. R. Paul, *Analysis of Multiconductor Transmission Lines*, 2nd ed. New York: Wiley, 2008.

[3] R. W. P. King, "Antennas in material media near boundaries with application to communication and geophysical exploration, Part I: The bare metal dipole," *IEEE Trans. Antennas Propag.*, vol. AP-34, no. 4, pp. 483–489, Apr. 1986.

[4] J. R. Wait, "The false image of a line current within a conducting half-space," *IEEE Trans. Electromagn. Compat.*, vol. 39, no. 3, pp. 266–267, Aug. 1997.

[5] M. Ramamoorty, M. M. B. Narayanan, S. Parameswaran, and D. Mukhedkar, "Transient performance of grounding grids," *IEEE Trans. Power Del.*, vol. 4, no. 4, pp. 2053–2059, Oct. 1989.

[6] Y. Liu, M. Zitnik, and R. Thottappillil, "An improved transmission-line model of grounding system," *IEEE Trans. Electromagn. Compat.*, vol. 43, no. 3, pp. 348–355, Aug. 2001.

[7] C. Mazzetti and G. M. Veca, "Impulse behavior of grounded electrodes," *IEEE Trans. Power App. Syst.*, vol. PAS-102, no. 9, pp. 3148–3156, Sep. 1983.

[8] A. Geri, "Behaviour of grounding systems excited by high impulse currents: The model and its validation," *IEEE Trans. Power Del.*, vol. 14, no. 3, pp. 1008–1017, Jul. 1999.

[9] S. S. Devgan and E. R. Whitehead, "Analytical models for distributed grounding systems," *IEEE Trans. Power App. Syst.*, vol. PAS-92, no. 5, pp. 1763–1770, Sep. 1973.

[10] R. Velazquez and D. Mukhedkar, "Analytical modeling of grounding electrodes," *IEEE Trans. Power App. Syst.*, vol. PAS-103, no. 6, pp. 1314–1322, Jun. 1984.

[11] L. Grcev and F. Dawalibi, "An electromagnetic model for transients in grounding systems," *IEEE Trans. Power Del.*, vol. 5, no. 4, pp. 1773–1781, Oct. 1990.

[12] L. Grcev and M. Popov, "On high-frequency circuit equivalents of a vertical ground rod," *IEEE Trans. Power Del.*, vol. 20, no. 2, pp. 1598–1603, Apr. 2005.

[13] R. Olsen and M. C. Willis, "A comparison of exact and quasi-static methods for evaluating grounding systems at high frequencies," *IEEE Trans. Power Del.*, vol. 11, no. 3, pp. 1071–1081, Jul. 1996.

[14] H. Rochereau and B. Merheim, "Application of the transmission lines theory and EMTP program for modelisation of grounding systems in high frequency range," Collection de notes internes, EDF-DER, Note 93NR00059, Paris, France, 1993.

Addition to "DC Internal Inductance for a Conductor of Rectangular Cross Section"

Ronald De Smedt

***Abstract*—The dc internal inductance of a conductor of elliptical cross section is used as a starting point to deduce, from numerically obtained results, approximate expressions for a conductor of rectangular cross section that are valid for any width and thickness.**

***Index Terms*—Inductance.**

I. Introduction

In the above paper [1], the dc internal inductance of a conductor of rectangular cross section was derived and calculated numerically. Among others, the results were fit to a polynomial expression as a function of the width w and thickness t of the rectangle. In this correspondence, we use the analytical result of an elliptical cross section as a starting point to deduce approximate expressions for a rectangular cross section that are now valid for any width and thickness.

II. Elliptical Cross Section

We start with the case of a conductor of elliptical cross section with semiaxes a and b. Due to its special shape, an analytical expression of the dc internal inductance (per unit length) can be derived (see the Appendix)

$$\frac{L_i}{\ell} = \frac{\mu}{8\pi}\frac{4ab}{(a+b)^2} = \frac{\mu}{8\pi}\frac{4ab}{a^2+2ab+b^2}. \tag{1}$$

From (1), we can immediately derive the expressions for a circular wire ($a = b$) and for a thin ellipse ($a \gg b$), respectively

$$\begin{aligned}\frac{L_i}{\ell} &= \frac{\mu}{8\pi}\times 1 \qquad (a=b)\\ &\approx \frac{\mu}{8\pi}\times\frac{4b}{a} \qquad (a \gg b).\end{aligned} \tag{2}$$

The asymptotic behavior of a thin ellipse—in particular, being proportional to the ratio of the smallest to the largest dimension—confirms a similar behavior found for a thin rectangle in [1, eq. (25)].

III. Rectangular Cross Section

Next, we consider the case of a conductor of rectangular cross section of width w and thickness t. In [1], it has been well elaborated how the dc internal inductance is derived and has to be calculated numerically. Use of careful and high-precision numerical quadrature allows obtaining a relative error of about 10^{-5}. For the further derivation and assessment of the approximated expressions (4) and (5), we have generated 301 values, logarithmically spread in the range $t/w = 1, \ldots, 10^{-6}$. In Table I, we present an excerpt of these results.

Manuscript received June 11, 2009; revised June 23, 2009. First published August 11, 2009; current version published August 21, 2009.

The author is with the Alcatel-Lucent Bell, Antwerp B-2018, Belgium (e-mail: ronald.de_smedt@alcatel-lucent.be).

Digital Object Identifier 10.1109/TEMC.2009.2027126

TABLE I
Numerical Values of L_i/ℓ Normalized to $\mu/8\pi$

Ratio t/w	Normalized L_i/ℓ	Ratio t/w	Normalized L_i/ℓ
1	0.96639	10^{-2}	$4.0325\cdot 10^{-2}$
0.5	0.85865	10^{-3}	$4.1670\cdot 10^{-3}$
0.2	0.53961	10^{-4}	$4.1860\cdot 10^{-4}$
0.1	0.32514	10^{-5}	$4.1885\cdot 10^{-5}$
0.03	0.11426	10^{-6}	$4.1887\cdot 10^{-6}$

First, we focus on two limiting cases: the square ($w = t$) (from Table I) and the thin rectangle ($w \gg t$) (from [1, eq. (25)])

$$\begin{aligned}\frac{L_i}{\ell} &= \frac{\mu}{8\pi}\times 0.96639 \qquad (w=t)\\ &\approx \frac{\mu}{8\pi}\times\frac{4\pi}{3}\frac{t}{w} = \frac{\mu}{8\pi}\times 4.1887902\frac{t}{w} \qquad (w \gg t).\end{aligned} \tag{3}$$

Compared to the elliptical configuration (2), we immediately note the similarity in the results. It also follows that the square has a somewhat lower inductance than the circle, and that the thin rectangle has a slightly larger inductance than a thin ellipse of the same ratio.

The similarity between the results of the ellipse and the rectangle now motivates us to propose a modification of the general expression (1) of the ellipse. We modify the coefficients "4" and "2" in (1) by forcing the value for a square and the behavior for thin rectangles, as given in (3), to arrive at

$$\frac{L_i}{\ell} \cong \frac{\mu}{8\pi}\frac{4.1888\ wt}{w^2 + 2.3345\ wt + t^2}. \tag{4}$$

Although only matched to the value of a square and the asymptotic behavior for thin shapes, the relative error of (4) with respect to numerical results (from which Table I is an excerpt) is less than 3.6% for *any* value of the width w and the thickness t.

We can further extend the expression (4) by adding new terms, while preserving both the necessary symmetry (so that w and t can be interchanged) and the behavior for thin rectangles

$$\frac{L_i}{\ell} \cong \frac{\mu}{8\pi}\frac{4.1888\ w^3t + 51.906\ w^2t^2 + 4.1888\ wt^3}{w^4 + 16.09\ w^3t + 28.2\ w^2t^2 + 16.09\ wt^3 + t^4}. \tag{5}$$

As in (4), two of the four degrees of freedom in (5) have been used to satisfy the limiting cases (3) exactly. The two remaining coefficients have been determined by minimizing the relative error for intermediate values of w and t at 301 values in the range $w/t = 1, \ldots, 10^{-6}$, which were obtained numerically (also see Table I). Compared to these results, the relative error of (5) is now less than 0.34% for *any* value of the width w and the thickness t. Further extensions of (5) with still higher powers of w and t are possible but do not give rise to substantial improvements.

The new expressions (4) and (5) have the advantage of being valid for the whole range of values of the width w and the thickness t, including the asymptotic behavior for thin shapes ($w \gg t$ and $w \ll t$).

Appendix

Internal Inductance of an Ellipse

To find an analytical solution for the dc magnetic field of a conductor of elliptical cross section that carries a constant current density, we make use of the elliptic cylinder coordinates [2]

$$\begin{cases} x = c\cosh\eta\,\cos\varphi \\ y = c\sinh\eta\,\sin\varphi \end{cases} \quad \text{with} \quad \begin{cases} 0 \le \eta < \infty \\ 0 \le \varphi \le 2\pi \end{cases} \tag{6}$$

where $c = \sqrt{a^2 - b^2}$ is the semifocal distance. The boundary of the ellipse is described by the constant $\eta = \eta_0$. The major and minor